iScience

CellPress
OPEN ACCESS

Article

Clock and riboswitch control of *THIC* in tandem are essential for appropriate gauging of TDP levels under light/dark cycles in Arabidopsis

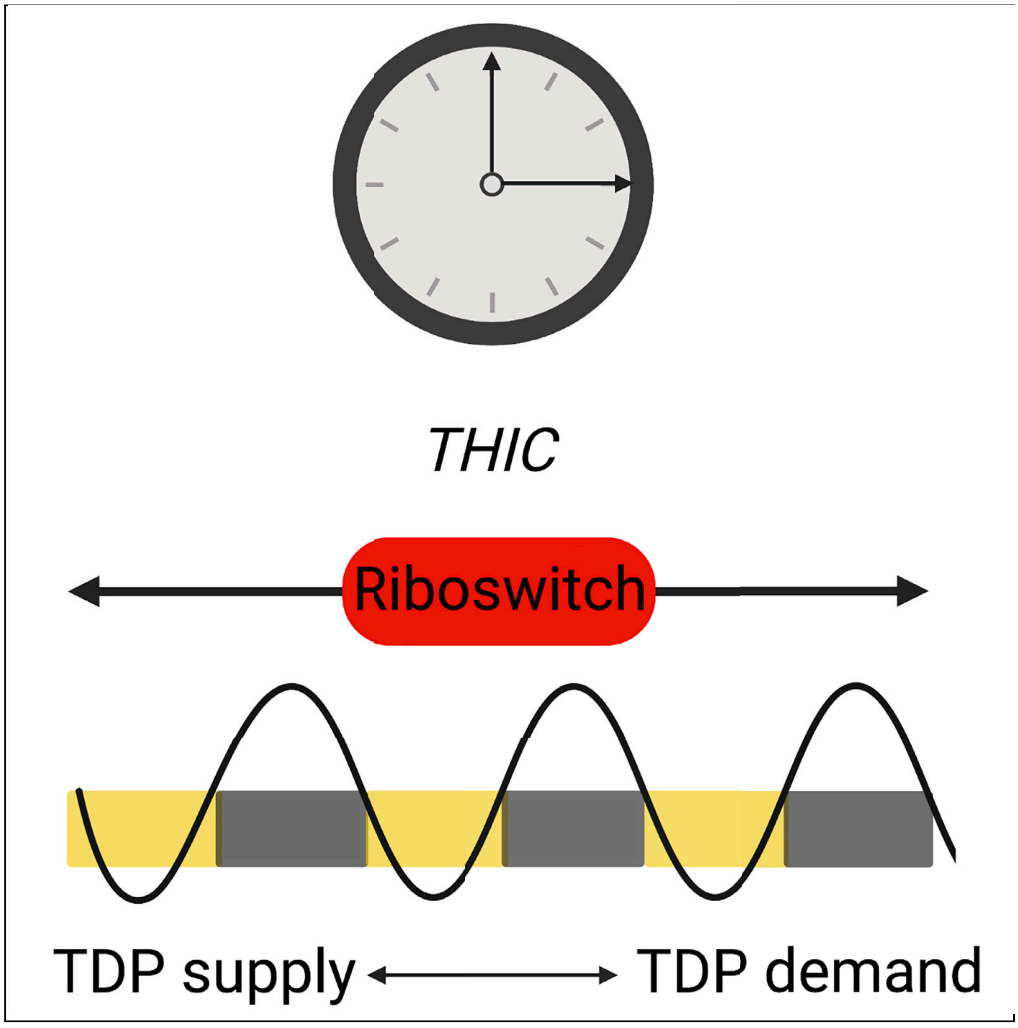

Zeenat Noordally, Lara Land, Celso Trichtinger, Ivan Dalvit, Mireille de Meyer, Kai Wang, Teresa B. Fitzpatrick

theresa.fitzpatrick@unige.ch

Highlights

We explore regulation of thiamine diphosphate levels in Arabidopsis

Time-of-day regulation of *THIC* expression is crucial under light/dark cycles

Temporal separation of TDP biosynthesis and transport allows for riboswitch precision

Coenzyme homeostasis within the well-studied domain of metabolic homeostasis is vital

Noordally et al., iScience *26*, 106134
March 17, 2023
https://doi.org/10.1016/j.isci.2023.106134

iScience

CellPress
OPEN ACCESS

Article

Clock and riboswitch control of *THIC* in tandem are essential for appropriate gauging of TDP levels under light/dark cycles in Arabidopsis

Zeenat Noordally,[1,2] Lara Land,[1,2] Celso Trichtinger,[1,2] Ivan Dalvit,[1] Mireille de Meyer,[1] Kai Wang,[1] and Teresa B. Fitzpatrick[1,3,*]

SUMMARY

Metabolic homeostasis is regulated by enzyme activities, but the importance of regulating their corresponding coenzyme levels is unexplored. The organic coenzyme thiamine diphosphate (TDP) is suggested to be supplied as needed and controlled by a riboswitch-sensing mechanism in plants through the circadian-regulated *THIC* gene. Riboswitch disruption negatively impacts plant fitness. A comparison of riboswitch-disrupted lines to those engineered for enhanced TDP levels suggests that time-of-day regulation of *THIC* expression particularly under light/dark cycles is crucial. Altering the phase of *THIC* expression to be synchronous with TDP transporters disrupts the precision of the riboswitch implying that temporal separation of these processes by the circadian clock is important for gauging its response. All defects are bypassed by growing plants under continuous light conditions, highlighting the need to control levels of this coenzyme under light/dark cycles. Thus, consideration of coenzyme homeostasis within the well-studied domain of metabolic homeostasis is highlighted.

INTRODUCTION

Central metabolism is under strict regulation to maintain homeostasis, requisite for health and fitness of all organisms. Key regulatory enzymes within the core metabolic pathways are assumed to generally deal with maintenance and adjust to address a challenge to homeostasis, the mechanisms of which remain to be fully elucidated.[1] A notable challenge exists in plants because the transitions between light and dark (L/D) periods require daily reprograming of metabolism, such that the alternation between the energy-generating process of photosynthesis during the day and its absence at night can be accommodated.[2] Indeed, several metabolites within the central pathways oscillate over diel cycles and are phased to particular times of the day,[3] implying daily regulation of enzyme activities. A large proportion of metabolic enzymes are dependent on organic coenzymes for activity. As the level of loading of the corresponding apoenzyme with the coenzyme dictates at least a pool of catalytic activity, the spatiotemporal provision of coenzyme could be hypothesized to contribute to enzyme-driven metabolic homeostasis to be *in sync* with daily L/D cycles.[4] However, this has been difficult to track because coenzyme biosynthesis pathways and their regulation need to be unraveled that in turn may provide the requisite tools. Moreover, studies on the significance of keeping coenzyme levels in check are lacking, and thus we remain uninformed on a whole facet of metabolic homeostasis and in turn plant health.

A major proportion of organic coenzymes are derived from B vitamins. Recently, the transcripts for biosynthesis and transport of B vitamin-derived coenzymes have been shown to be strongly time-of-day regulated in plants.[4] One of the most tightly regulated is the coenzyme thiamine diphosphate (TDP) derived from vitamin B_1 for which biosynthesis and transport are phased to different times of the day.[5] Key regulatory enzyme nodes of central metabolism are dependent on TDP as a coenzyme (Figure S1), among which are pyruvate dehydrogenase (glycolysis, Krebs cycle), α-ketoglutarate dehydrogenase (Krebs cycle, amino acid metabolism), transketolase (pentose phosphate pathway and Calvin cycle), and acetolactate synthase (branched chain amino acid synthesis). Interestingly, TDP is short-lived (estimated half-life 10 h[6]) and can be destroyed during enzymatic catalysis,[7] that drives a high rate of biosynthesis (0.1 nmol h^{-1} g^{-1} in leaves[6]). Biosynthesis involves the suicide enzyme THIAMIN 1 (THI1) (Figure S1) that donates a peptide backbone sulfur atom to the TDP molecule, rendering THI1 non-functional in this context after a single catalytic cycle.[8]

[1]Vitamins and Environmental Stress Responses in Plants, Department of Plant Sciences, University of Geneva, 1211 Geneva, Switzerland

[2]These authors contributed equally

[3]Lead contact

*Correspondence: theresa.fitzpatrick@unige.ch

https://doi.org/10.1016/j.isci.2023.106134

This results in a remarkably high turnover rate of THI1 (one of the fastest known[9]) that is estimated to consume 2-12% of the maintenance energy budget in plants.[10] Therefore, it is thought that luxurious supply of TDP does not occur in plants;[11] rather, it is made as needed. Coordination of supply to meet demand implies strict monitoring of TDP levels that are intertwined with metabolic requirements. In line with this, TDP levels are monitored in the nucleus by a riboswitch—the only known example in plants.[12] The riboswitch operates by alternative splicing in the 3′-UTR of the biosynthesis gene *THIAMIN C* (*THIC*)[13,14] as a function of TDP levels (Figures S1 and S2A). Engineering of a dysfunctional riboswitch in Arabidopsis results in plants that are chlorotic and stunted in growth and is interpreted to be due to excessive levels of TDP that occur in these plants.[15] Interestingly, riboswitch mutant plants are unable to adapt to a change in photoperiod,[3] suggesting that the riboswitch is particularly important under L/D cycles. However, this has not been explored further and could be important in terms of plant fitness. More generally, the characteristics of TDP and its regulation provide an opportunity to explore the importance of daily surveillance of coenzyme levels.

Here we show that Arabidopsis plants can accommodate modestly enhanced levels of TDP, as long as it is managed appropriately. In particular, control of *THIC* transcript levels is critical and should be phased to the evening under L/D cycles managed by the circadian clock and the *THIC* riboswitch in tandem. Disrupting the response to TDP status leads to a fitness penalty under L/D cycles that can be bypassed by growing plants under persistent light (L/L).

RESULTS AND DISCUSSION

Modestly enhanced tissue levels of TDP *per se* do not account for the growth defect in Arabidopsis riboswitch mutants

In a previous study,[15] riboswitch mutant lines were generated in the SALK_011114 background (named here as *thiC1-2*, Table S1) that has a transfer DNA (T-DNA) insertion in the promoter of *THIC* leading to reduced *THIC* expression.[16] Specifically, *thiC1-2* transgenic lines carrying either the *pTHIC:THIC:RR* or *pTHIC:THIC:NRR* construct expressing *THIC* under the control of its own upstream region and either the native 3′-UTR (termed here as responsive riboswitch [*RR1*]) or a non-functional version of the 3′-UTR carrying an A515G mutation relative to the *THIC* stop codon (termed here as non-responsive riboswitch [*NRR1*]), respectively, were produced (Figure S2A and Table S1).[15] Here, we assessed the performance of a newly generated set of riboswitch mutant lines using the same strategy as before but in the original null allele of *thiC* (SAIL_793_H10) referred to here as *thiC1-1* (Figure S2A and Table S1), which has an T-DNA insertion in the third intron of *THIC*.[17] We refer to the new lines as *NRR2* and *RR2* (Table S1). For comparison with regards to TDP content, we also included engineered lines expressing *THIC* and *THI1* under the control of the *UBQ1* and *CaMV 35S* constitutive promoters and the *UBQ1* and *OCS* terminators, respectively, in wild-type Col-0 (referred to here as *TTOE*) (Figure S2A and Table S1). Similar to *NRR1*, *TTOE* are reported to have TDP levels above wild type.[18] We compared the phenotypic morphology of these lines under three different photoperiod regimes, 8 h, 12 h, or 16 h of light. The newly generated *NRR2* lines were chlorotic and had a small leaf lamina with only ca. 50% leaf coverage compared to wild type (Figure 1A) and reduced biomass (Figure 1B). This corroborates previous observations with *NRR1* in the *thiC1-2* background,[15] and thus they can be considered morphologically equivalent. However, whereas the phenotype of *NRR* lines persists under all three photoperiods, the *TTOE* lines were morphologically similar to wild type and with equivalent biomass (Figures 1A and 1B). To test if a pronounced difference in TDP levels could explain the difference between *NRR1/2* and *TTOE*, we measured TDP content by an established high-performance liquid chromatography (HPLC) protocol.[5,19] The *NRR1/2* lines showed a significant increase in TDP over wild type (Figure 1C) as reported previously,[15] albeit modest; however, the level of TDP in the *TTOE* lines was higher than that in the other lines (Figure 1C). Although the levels of thiamine were also significantly increased in *TTOE* lines (Figure S3), these observations suggested that the level of TDP *per se* does not account for the chlorotic, stunted growth phenotype observed in *NRR* lines.

Balancing thiamine pathway deficits does not salvage improper *THIC* expression levels

In addition to being under riboswitch control, *THIC* transcript levels are strongly influenced by the circadian clock. In particular, an evening element is found in the promoter sequence of *THIC* (Figures S1 and S2A) that can bind the morning-expressed Myb-like transcription factors CIRCADIAN CLOCK ASSOCIATED 1 (CCA1) or LATE ELONGATED HYPOCOTYL (LHY) and is reported to repress transcription early in the day.[15,20,21] In line with this, transcript levels of *THIC* peak in the evening.[5,15] We measured *THIC* transcript abundance in representatives of our set of lines grown for 4 weeks under equinoctial conditions (LD 12:12

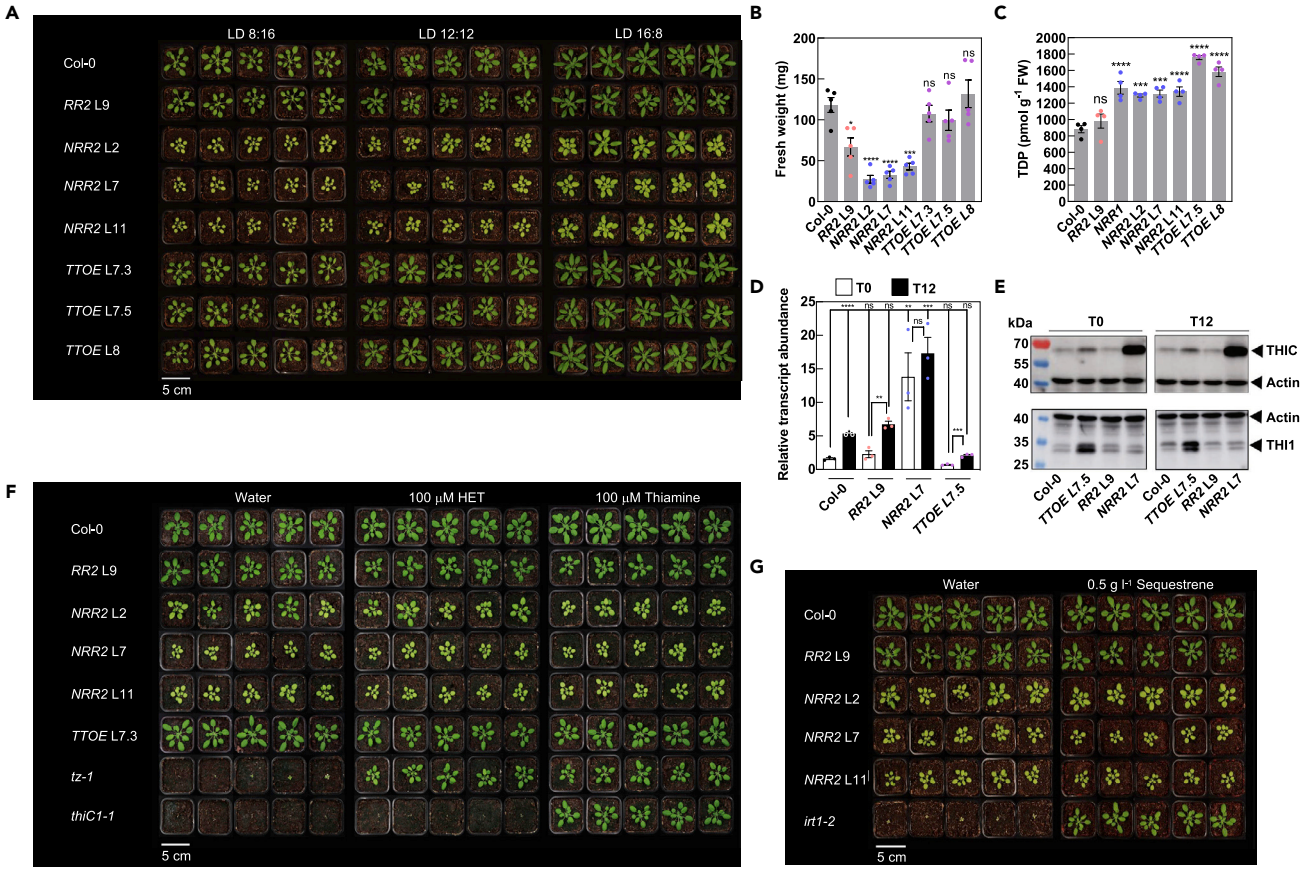

Figure 1. Enhanced TDP content *per se* does not explain the severe phenotype of *THIC* riboswitch mutant plants

(A) Rosette morphology of Col-0 (wild-type) Arabidopsis plants compared to transgenic lines in the *thiC1-1* background carrying the wild type (*RR2*) or mutated riboswitch (*NRR2*) and *THIC THI1* overexpressor (*TTOE*) lines in the Col-0 background. Plants were grown on soil under 8, 12, or 16 h photoperiods (120–140 µmol m^{-2} s^{-1} white light) and the corresponding dark period to reach a 24 h cycle (LD 8:16, LD 12:12, LD 16:8, respectively) and a constant temperature of 20°C. Photos were taken 35 days after germination (DAG) for LD 8:16 and 28 DAG for LD 12:12 and LD 16:8.

(B) The fresh weight biomass of shoot material of lines as in (A) grown under LD 12:12 and harvested 28 DAG at 8 h into the photoperiod. Data represent means of four biological replicates each consisting of a pool of five plants, the standard error of the means (SEM), and one-way ANOVA significance with respect to Col-0.

(C) TDP levels of lines as in (B) as well as *NRR1* in the *thiC1-2* background.

(D) Expression of *THIC* CDS by RT-qPCR in lines as indicated, grown as in (B) but harvested before the onset of light (T0, white bars) and before the onset of dark (T12, black bars). Transcript levels were normalized to *UBC21*. Data represent means of three biological replicates each consisting of a pool of five plants and the standard error of the means (SEM). The statistical significance of the variables of time was assessed with a *t*-test and genotype with one-way ANOVA and comparison to Col-0.

(E) Immunochemical analyses of THIC and THI1 protein abundance at T0 and T12, with actin as a loading control of plant samples as in (D). Total extracted protein was separated on 12% 37.5:1 polyacrylamide gels.

(F) Plants were grown as in (B) and watered and sprayed twice a week with either water or 100 µM hydroxyethylthiazole (HET) or 100 µM thiamine. The mutant lines *tz-1* (cannot make HET) and *thiC1-1* were used as controls for HET and thiamine rescue, respectively.

(G) Plants were grown as in (B) and watered and sprayed twice a week with either water or 0.5 g L^{-1} Sequestrene. The *irt1-2* mutant (impaired in iron transport) was used as a control for iron availability.In all cases, significance values are noted as **** for $p \leq 0.0001$, *** for $p \leq 0.001$, * for $p \leq 0.05$ and ns for not significant.

cycles), at the onset of light (T 0) and at the onset of dark (T 12). Transcript levels of *THIC* were more abundant at T 12 in wild type (Figure 1D), corroborating earlier reports.[5,15] A similar pattern was observed in the *RR* line—the complemented *thiC* carrying an intact riboswitch (Figure 1D). On the other hand, the *NRR* line—*thiC* carrying a dysfunctional riboswitch—showed increased abundance of *THIC* transcript both in the morning and the evening, i.e., constitutive overexpression (Figure 1D). Our data also indicate that time-of-day control of *THIC* expression is lost (Figure 1D), despite the transgene carrying the upstream region of *THIC* that harbors the evening element (Figure S2A). Surprisingly, on the other hand, in *TTOE*,

although expression of the *THIC* transgene is under control of the constitutive *UBQ1* promoter and terminator, total *THIC* transcript levels (i.e. endogenous and transgene) were not significantly different from that in wild type (Figure 1D). Moreover, an increased accumulation at T 12 compared to T 0 was observed similar to wild type (Figure 1D). Thus, time-of-day control of *THIC* transcript levels appears to be intact in *TTOE*, which is in the wild-type background and thus has a functional endogenous riboswitch. As the level of THIC protein was not examined in previous studies, we also performed immunodetection of THIC in the same samples using an antibody raised against the Arabidopsis protein.[17] Interestingly, the level of THIC protein was considerably more abundant in *NRR* compared to any of the other lines, while the level in *TTOE* was only slightly higher than that in either wild type or *RR* (Figure 1E). It has previously been demonstrated that a balance is achieved (and necessary) between the key enzymes of TDP biosynthesis, THIC and THI1 (Figure S1), to furnish equal provision of the pyrimidine and thiazole heterocycle precursors, respectively, of the TDP molecule.[22–24] Thus, we tested the level of THI1 protein in our lines using a peptide antibody raised against the Arabidopsis protein.[18] Although the level of THI1 was increased in *TTOE* as would be expected, there was no significant difference among the other lines (Figure 1E). The higher level of TDP in *TTOE* compared to *NRR* might be accounted for by enhanced expression of both THIC and THI1 in *TTOE*, whereas the loss of negative feedback on *THIC* expression in NRR leads to a more modest increase as THI1 would be limiting. Given the higher abundance of THIC protein in *NRR* and its strong phenotype compared to wild type or *TTOE*, we next tested if supplementation with the thiazole moiety, hydroxyethylthiazole (HET—the product of the THI1 reaction), would compensate for a possible imbalance in the provision of the pyrimidine moiety by THIC. Although HET supplementation rescued the strong growth defects observed in the *THI1* mutant, *tz-1*[25] (Table S1), it did not improve growth of *NRR* (Figure 1F). Supplementation with thiamine itself rescues both *thi1 (tz-1)* and *thiC* mutant lines as expected but had no effect on the *NRR* phenotypes (Figure 1F). This suggests that an imbalance in the provision of the thiazole and pyrimidine moieties is not responsible for the phenotype in *NRR*. Of notable interest is that immunodetection of THI1 results in two bands that may represent two different forms of the protein targeted to either plastids or mitochondria.[26] The higher-mobility band is relatively less abundant in the evening in all lines, and the lower mobility band is more abundant in the evening relative to the morning (Figure 1E). This suggests daily regulation of the THI1 protein. Next, as the holoenzyme form of THIC carries an iron-sulfur cluster necessary for both stability and activity,[17] it is also plausible that overaccumulation of THIC may divest other proteins of this necessary cofactor. Notable among iron-sulfur cluster proteins are those of photosynthesis and proteins involved in chlorophyll biosynthesis.[27] Moreover, chlorosis, as seen in *NRR*, is a diagnostic feature of iron deficiency.[28] We therefore tested if iron supplementation could improve the growth of *NRR* on the assumption that assembly of iron-sulfur clusters is not impaired in *NRR* and sulfur is not limiting. Whereas watering with Sequestrene (Fe-EDDHA) restored growth to the *IRON-REGULATED TRANSPORTER1* (*irt1-2*) mutant[29] (Table S1), which in the absence of iron supplementation is stunted in growth and chlorotic, it did not improve growth of *NRR* (Figure 1G).

Taken together, our data show that while TDP levels are increased in both *NRR* and *TTOE*, control of *THIC* expression is different. Regulation of *THIC* transcripts is abolished in *NRR* (despite the presence of clock-controlled elements in the promoter of the transgene), while *TTOE* mimics wild type suggesting a complex interaction of the clock and riboswitch in *THIC* transcript control with the riboswitch having a dominant effect.

Loss of regulation of *THIC* expression in riboswitch mutants is not due to impaired clock function, although TDP impacts clock features

The loss of regulation of *THIC* expression drew our attention to the circadian clock, and we were next prompted to test if the circadian clock is deregulated in these transgenic lines. We assessed for clock activity by measuring transcript abundance of the reporter gene *CHLOROPHYLL A/B BINDING 2* (*CAB2*)[30,31] by quantitative RT-PCR (RT-qPCR) from plants maintained under equinoctial (LD) conditions sampling every 4 h for 72 h. An initial visualization of the transcript distributions did not reveal any striking differences between *NRR* or *TTOE* compared to wild type (Figure 2A). Notably, the robust daily rhythm of *CAB2* expression upon entrainment was maintained under continuous light (free-running) conditions in all lines but abolished in the arrhythmic circadian clock mutant of PSEUDO RESPONSE REGULATOR proteins 5, 7, and 9 (*prr5 prr7 prr9*, Table S1) under free-running and LD[32] (Figure S4). We also measured key morning- and evening-phased components of the genetically encoded circadian clock, *CCA1* and *TIMING OF CAB EXPRESSION1* (*TOC1*), respectively, as well as the day-phased constituents *PRR7* and *PRR9* under LD (Figure 2A). In all cases, we assessed period, phase, and amplitude using Biodare2 (https://biodare2.ed.ac.uk/)[33] and found

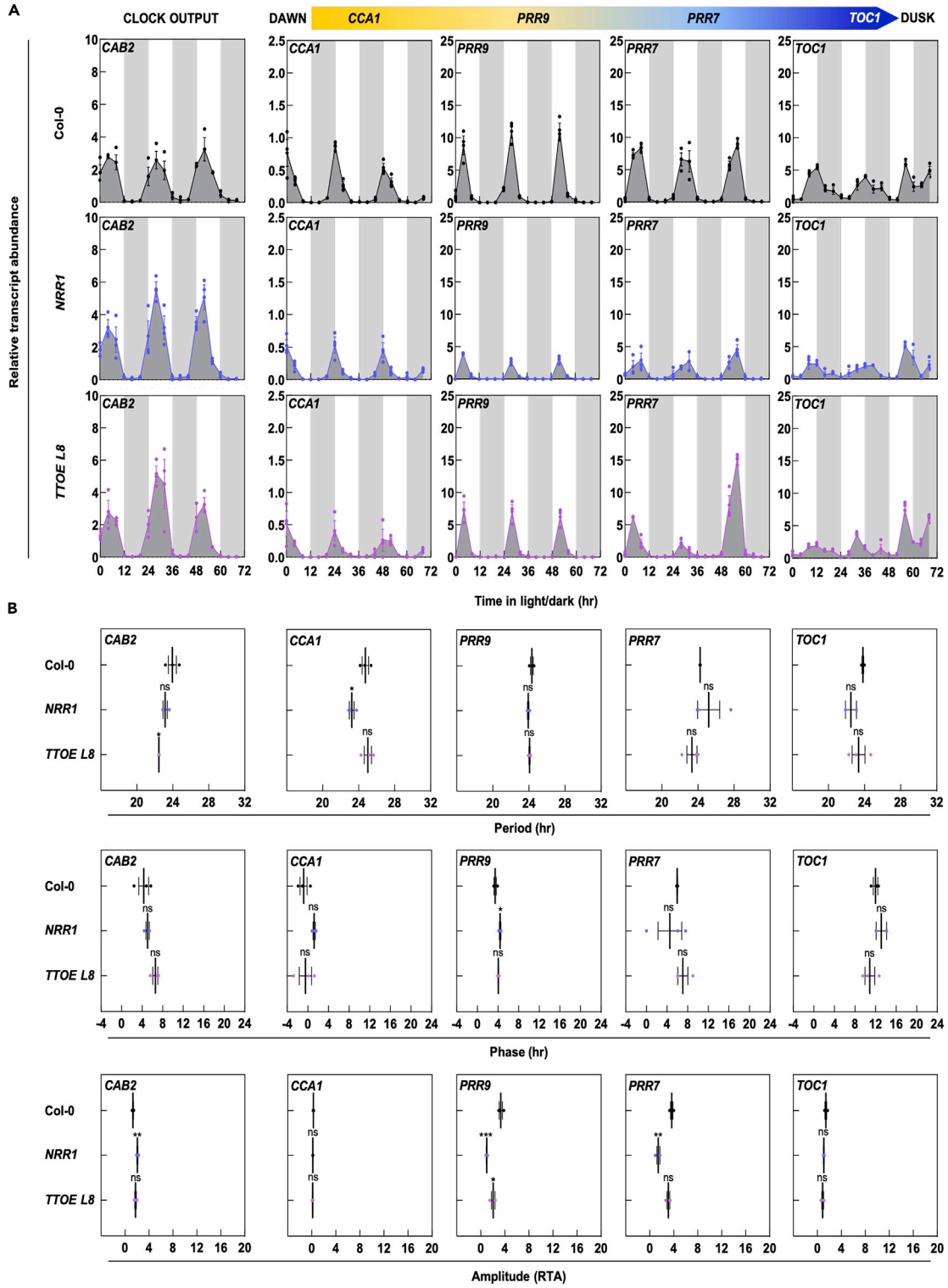

Figure 2. Performance of the clock in lines altered in TDP contents and its sensing

(A) Transcript abundance of clock genes *CCA1*, *PRR7*, *PRR9*, and *TOC1* that progressively peak from dawn to dusk and the clock reporter gene *CAB* by RT-qPCR in Col-0 (wild-type, black), mutated riboswitch (*NRR1*, blue), and *THIC THI1* overexpressor (*TTOE*, purple) lines. Plants were grown in culture on ½ MS agar plates under a 12 h photoperiod (120 μmol photons m^{-2} s^{-1} white light) and 12 h of darkness at a constant temperature of 20°C. Shoot material was harvested 14 days after germination from pooled seedlings (n = 10) every 4 h at the times indicated. White and gray background bars represent day and

Figure 2. *Continued*

night, respectively. Data of three individual experimental replicates of pooled material are shown with error bars representing SEM. Transcript levels are relative to *UBC21*.

(B) Period, phase, and amplitude (relative transcript abundance, RTA) estimates of gene expression of the Arabidopsis lines in (A) based on the maximum entropy spectral analysis (MESA) algorithm in BioDare2. Data of three individual experimental replicates are shown with the mean (black line) and error bars representing SEM. Significance values are noted as *** for $p \leq 0.001$, * for $p \leq 0.05$ and ns for not significant, calculated by one-way ANOVA followed by Tukey's multiple comparisons test.

that neither period nor phase deviated considerably from wild type, although there were subtle differences in period and phase of *CCA1* and *PRR9* transcripts, respectively, in *NRR* (Figure 2B). The amplitude of *PRR9* was decreased in *NRR* and *TTOE*, and that of *PRR7* was decreased in *NRR* (Figure 2B). This implies that the molecular clock is largely operational and near normal in all lines under LD albeit with a reduced amplitude of transcript levels of some components in both *NRR* and *TTOE*. Given that both of the latter have enhanced levels of TDP in common, this suggests that elevated TDP may influence the level of activity of components of the molecular oscillator at least at the transcriptional level. Nonetheless, the data do not support a hypothesis that altered performance of the circadian clock accounts for the stark differences in morphology and daily control of *THIC* expression between *NRR* and *TTOE* and was thus not explored further in the context of this study.

Sensing of TDP levels is crucial under L/D cycles but not continuous light

As mentioned above, the supply of TDP is presumed to be coincident with demand by enzymes dependent on it as coenzyme such that over- or under-supply does not negatively impact plant fitness.[6,11] Such tight regulation is postulated to contribute to homeostasis and the natural metabolic reprograming that occurs in plants between day and night cycles.[4,15] Support for this comes from the recent observation of daily oscillations of free TDP levels that reflects metabolic differences at the cellular level under L/D cycles and represents the divergence from supply of TDP and the cellular demand by apoenzymes on a daily basis, even though tissue levels of TDP do not change.[5] Thus, the riboswitch is expected to be crucial for monitoring cellular levels of TDP and ensuring an appropriate response in line with changes perceived. Therefore, a gauged response from the endogenous riboswitch in *TTOE* might be sufficient to account for the time-of-day regulation of *THIC* expression therein and thus the ability to deal with the enhanced tissue levels of TDP. *NRR* on the other hand would not be able to perceive or transmit alteration of cellular TDP levels due to a non-functional riboswitch. In order to test riboswitch functionality, we monitored splicing of the second intron in the 3′-UTR of *THIC* (referred to as intron spliced, *IS*) (Figure 3A), which acts as a proxy for the response to TDP levels,[5] for 72 h under equinoctial conditions across all lines. Firstly, in wild type, a distinct strong daily rhythm in the abundance of *IS* reflecting the daily oscillation of TDP levels is observed (Figure 3A), corroborating a previous study.[5] As expected in *NRR*, overall transcript levels of *IS* are low, and no robust oscillation can be discerned, in line with the impaired splicing (Figure 3A). On the other hand, in *TTOE*, there is a strong robust rhythm of *IS* that has an increased amplitude compared to wild type (Figure 3A [note scale difference] and B). As *IS* responds directly to free TDP levels, the increase in *TTOE* suggests perception and response to the higher TDP levels in this line. Splicing of the second intron in the 3′-UTR of *THIC* was confirmed in wild type and *TTOE* as amplification of this region reveals a fragment size of 120 bp (corresponding to splicing of intron 2), while a fragment size of 272 bp is observed for *NRR* corresponding to retention of the second intron (Figure S5A). Furthermore, maintenance of the daily oscillation of *IS* in the arrhythmic *prr5 prr7 prr9* mutant[32] and loss of *IS* oscillation under constant light (LL) conditions suggest the *IS* rhythm is responding to TDP as a function of L/D cycles (Figure S5B), corroborating an earlier study.[5]

Our data imply that enhanced levels of TDP can be accommodated in Arabidopsis as long as a functional riboswitch is present. With this information in hand, we hypothesized that while gauging of TDP levels by the riboswitch is important for fitness performance under L/D cycles, its requirement can likely be bypassed under LL during which a response to adjustment of TDP levels is less important as daily metabolic reprograming coincident with L/D does not occur. We therefore checked growth of all lines under LL and indeed did not observe any morphological difference or significant change in biomass between them (Figures 3C and 3D), notably for *NRR* which is in stark contrast to its performance under L/D cycles. Thus, the morphological defect resulting from the non-functionality of the riboswitch can be bypassed by growing plants under LL. Furthermore, the increased expression of *THIC* (transcript and protein) is still observed in *NRR* indicating that this can be tolerated in LL (Figure 3E).

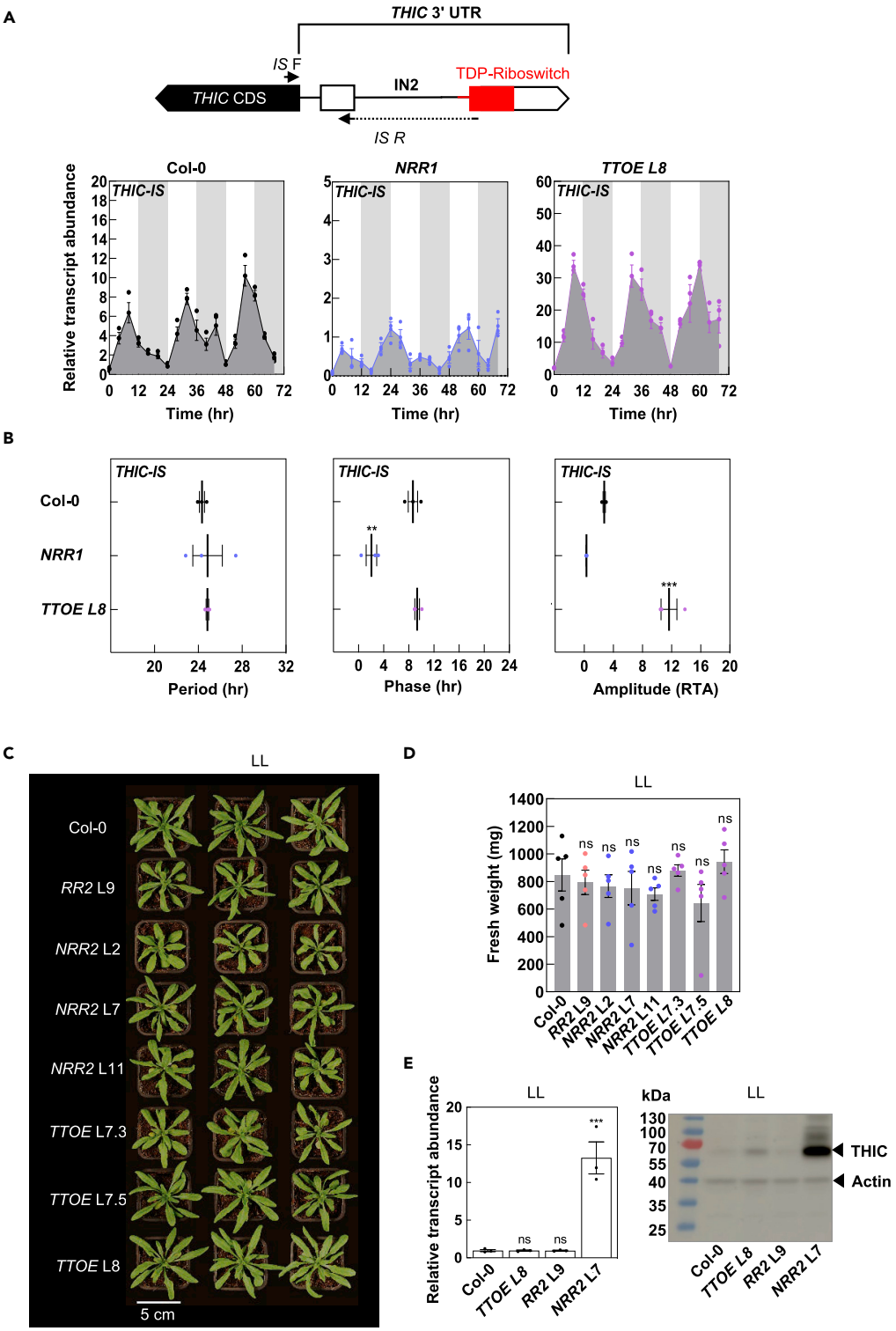

Figure 3. Riboswitch requirement can be bypassed under continuous light

(A) Gene model of part of *THIC*. The coding sequence (CDS; black box), two exons in the 3′-UTR (white boxes), introns as black lines and the riboswitch (red box) are depicted. The abundance of the transcript in which the second intron (IN2) has been spliced (*IS*) is monitored using the *IS* F and *IS* R primers and gauges the response of the riboswitch to TDP. *IS* R (solid black line) spans the spliced site as shown. Transcript abundance of *IS* variants of *THIC* by RT-qPCR. Plants were grown in

Figure 3. *Continued*

culture on ½ MS agar plates under a 12 h photoperiod (120 μmol photons m^{-2} s^{-1} white light) and 12 h of darkness at a constant temperature of 20°C. Shoot material was harvested 14 days after germination from pooled seedlings (n = 10) every 4 h at the times indicated. White and gray background bars represent day and night, respectively. Data of three individual experimental replicates of pooled material are shown (note scale differences) with error bars representing SEM. Transcript levels are relative to *UBC21*.

(B) Period, phase, and amplitude (relative transcript abundance, RTA) estimates of gene expression of the Arabidopsis lines in (A) based on the Maximum Entropy Spectral Analysis (MESA) algorithm in BioDare2. Data of three individual experimental replicates are shown with the mean (black line) and error bars representing SEM. Significance values are noted as *** for $p \leq 0.001$, ** for $p \leq 0.01$, calculated by one-way ANOVA followed by Tukey's multiple comparisons test.

(C) Rosette morphology of Col-0 (wild-type) Arabidopsis plants compared to transgenic lines carrying the wild type (*RR*) or mutated riboswitch (*NRR*), or overexpression of *THIC* and *THI1* (*TTOE*). Plants were grown on soil under continuous light (LL, 120 to 140 μmol m^{-2} s^{-1} white light) and a constant temperature of 20°C. Photos were taken 28 days after germination.

(D) The fresh weight biomass of shoot material of lines as in (C). Data represent means of five biological replicates each consisting of a pool of five plants, error bars represent SE, ns for not significant with respect to Col-0 calculated by one-way ANOVA.

(E) Expression of *THIC* CDS by RT-qPCR (left panel) or immunochemical analysis (right panel) in lines as indicated, grown as in (C) harvested at 8 a.m. CET. Transcript levels were normalized to *UBC21*. RT-qPCR data represent means of three biological replicates each consisting of a pool of five plants and the standard error of the means (SEM), and significance was calculated by one-way ANOVA followed by a Dunnett's multiple comparison test with respect to Col-0. For immunochemical analyses actin was used as a loading control. Total extracted protein (20 μg) was separated on 12% 37.5:1 polyacrylamide gels.

Taken together, acute sensing of TDP levels through the *THIC* riboswitch suggests its coordination with daily regulation of *THIC* transcript levels. The higher TDP levels appear to be sensed in *TTOE* and are accommodated through increased alternative splicing of (presumably endogenous) *THIC*, which adjusts overall transcript levels to approximate the behavior of wild type. On the other hand, sensing of TDP levels is disrupted in *NRR*, and it is ineffective in regulation of *THIC* expression levels. Thus, modestly enhanced levels of TDP can be accommodated in the presence of a functional riboswitch. Notably, the riboswitch is responding to free TDP levels in the nucleus; how other subcellular organelle TDP level status is transmitted to the riboswitch is unknown.

Correct phasing of *THIC* expression is critical to plant fitness

We postulated that *THIC* expression is coupled to the requirement for TDP under L/D cycles and is gauged by the riboswitch. In parallel, the circadian clock anticipates time-of-day appropriate control, with peak *THIC* expression in the evening. Notably, transcripts for known organellar transport of TDP such as *NUCLEOBASE CATION SYMPORTER1* (*NCS1*) and *THIAMINE PYROPHOSPHATE CARRIER1* (*TPC1*) are temporally separated from those of *THIC* and peak in the morning.[5] To test if phasing of *THIC* expression is important and thus temporal separation of TDP biosynthesis and transport, we next designed a strategy to synchronize transcript abundance of both processes to the same time of day. As several transporters are implicated in TDP transport,[34] the simplest way to engineer this experiment was to phase the peak in expression of the biosynthesis gene *THIC* to the morning (instead of its natural peak in the evening) to be coincident with the peak in abundance of known TDP transporters (around ZT 1-2).[5] To facilitate this, we used two approaches. On the one hand, we placed *THIC* expression under control of the *ACYL CARRIER PROTEIN 4* (*ACP4*) promoter that is phased to ZT 0-2 and shows similar levels of expression to *THIC* in microarray data (Figure S6). For the second approach, we mutated the promoter located evening element (AAATATCT) in *THIC* to the CIRCADIAN CLOCK ASSOCIATED 1-binding site (CBS) element (AAAAATCT) that has previously been shown to change the phase of evening-expressed transcripts to the morning[35] (Figure S2B). These constructs *pACP4:THIC* and *pTHIC_EE_CBS:THIC*, both of which carried the 3′-UTR of *THIC* and therefore the riboswitch, were introduced into *thiC1-1* (Figure S2B and Table S1). Lines homozygous for the respective construct were assessed for time-of-day *THIC* expression under LD. Indeed, the transcript expression levels of *THIC* in *pACP:THIC* almost match those of wild type but are phased to the morning rather than the evening (Figure 4A). Transcript expression levels of *THIC* are phased to the morning rather than the evening also in *pTHIC_EE_CBS:THIC*, although the overall levels are significantly higher than in *pACP:THIC* or wild type, suggesting that this mutation also promotes transcript expression (Figure 4A). Importantly, transcripts of known TDP transporters *NCS1* and *TPC1* were still phased to the morning in these lines and are thus coincident with the expression of *THIC* (Figure S7). Notably, THIC protein levels were increased significantly in *pTHIC_EE_CBS:THIC* and to a lesser extent

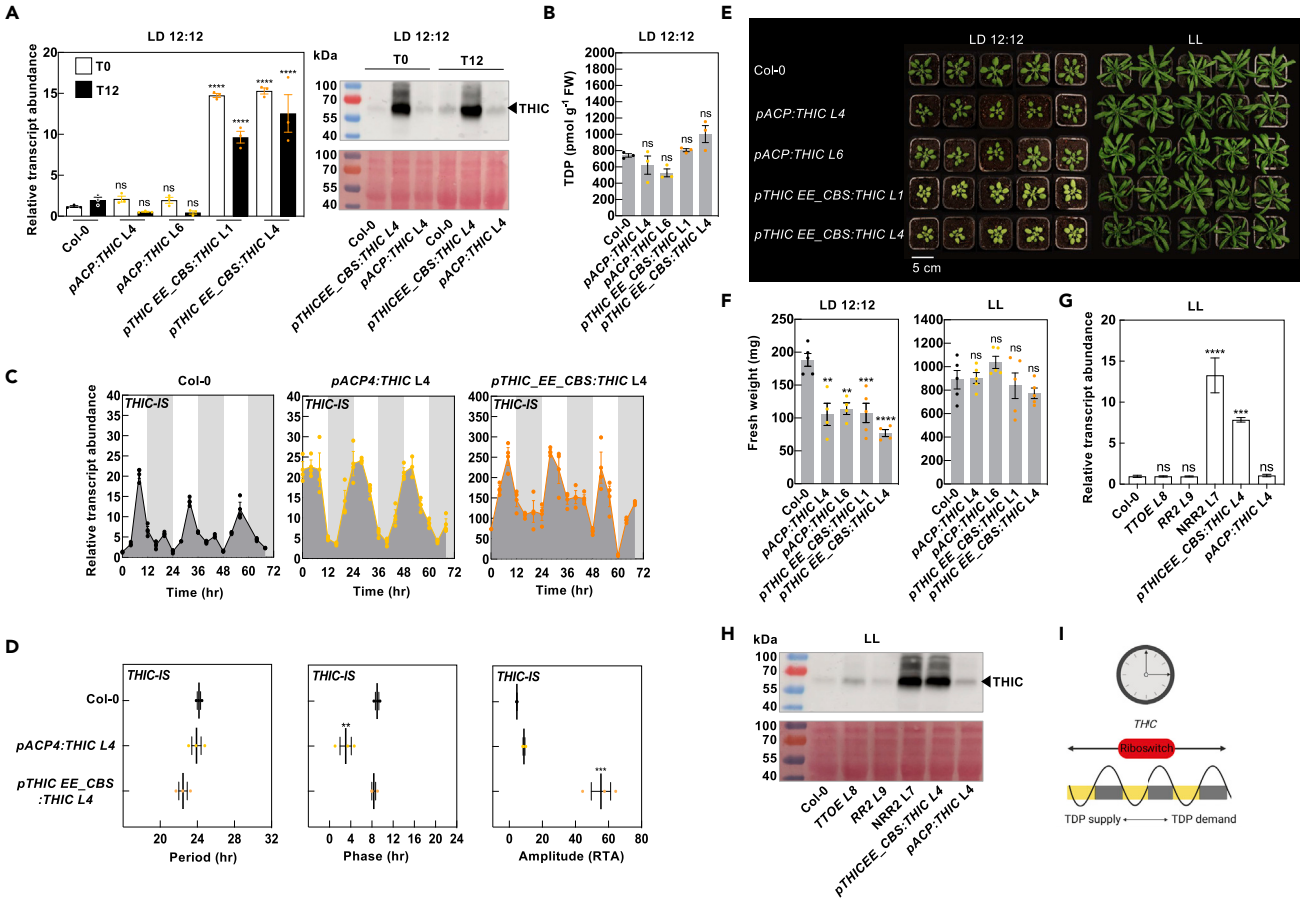

Figure 4. Phasing of *THIC* expression is important under light/dark cycles

(A) The left panel shows transcript levels of *THIC* CDS in Col-0 (wild type) compared to transgenic lines in which *THIC* expression is either under control of the promoter of *ACYL CARRIER PROTEIN4* (*ACP4*, *pACP4:THIC*) or in which the *THIC* promoter-based evening element (EE) has been mutated to the *CIRCADIAN CLOCK ASSOCIATED 1*-binding site (CBS, *pTHIC EE_CBS:THIC*). Transcripts levels were normalized to *UBC21*. Data represent means of three biological replicates each consisting of a pool of five plants, the standard error of the means (SEM), and one-way ANOVA significance with respect to either T0 or T12 in Col-0, where significance values are noted as **** = $p \leq 0.0001$ and ns for not significant are indicated. The right panel shows immunochemical staining of THIC in samples shown on the left. Ponceau S staining indicates protein loading (20 mg total) and were separated on 12% 37.5:1 polyacrylamide gels. Plants were grown under a 12 h photoperiod (120 μmol photons m^{-2} s^{-1} white light) and 12 h of darkness at a constant temperature of 20°C, harvested 28 days after germination (DAG) before the onset of light (T0, white bars) and before the onset of dark (T12, black bars).

(B) TDP levels of lines as in (A).

(C) Transcript abundance of 3′-UTR second intron spliced (*IS*) variants of *THIC* by RT-qPCR. Plants were grown in culture on 1/2 MS agar plates under a 12 h photoperiod (120 μmol photons m^{-2} s^{-1} white light) and 12 h of darkness at a constant temperature of 20°C. Shoot material was harvested 14 DAG from pooled seedlings (n = 10) every 4 h at the times indicated. White and gray background bars represent day and night, respectively. Data of three individual experimental replicates of pooled material are shown with error bars representing SEM. Transcript levels are relative to *UBC21*.

(D) Period, phase, and amplitude (relative transcript abundance, RTA) estimates of gene expression of the Arabidopsis lines in (C) based on the maximum entropy spectral analysis (MESA) algorithm in BioDare2. Data of three individual experimental replicates are shown with the mean (black line) and error bars representing SEM. Significance values are noted as *** for $p \leq 0.001$, ** for $p \leq 0.01$, calculated by one-way ANOVA followed by Tukey's multiple comparisons test.

(E) Rosette morphology of lines as in (A) grown on soil under a 12 h photoperiod (120–140 μmol m^{-2} s^{-1} white light) and 12 h of darkness (LD 12:12) or continuous light (LL) and a constant temperature of 20°C. Photos were taken 28 DAG.

(F) The fresh weight biomass of shoot material of lines as in (E). Data represent means of four biological replicates each consisting of a pool of five plants, the standard error of the means (SEM), and one-way ANOVA significance with respect to Col-0.

(G) Transcript levels of *THIC* CDS in Col-0 (wild-type) compared to transgenic lines as indicated. Transcripts levels were normalized to *UBC21*. Data represent means of three biological replicates each consisting of a pool of five plants, the standard error of the means (SEM), and one-way ANOVA significance with respect to Col-0, where significance values are noted as **** = $p \leq 0.0001$, *** = $p \leq 0.001$ and ns for not significant are indicated. Plants were grown under continuous light (LL) (120 μmol photons m^{-2} s^{-1} white light) and a constant temperature of 20°C, harvested 28 DAG at 8 a.m. CET.

(H) Immunochemical staining of THIC in samples shown in (G). Ponceau S staining indicates protein loading (20 μg total) and were separated on 12% 37.5:1 polyacrylamide gels.

Figure 4. *Continued*

(I) Proposed working model for integration of TDP supply and demand over light dark cycles (yellow and dark rectangles, respectively) as a function of the circadian clock control. In addition, levels of free TDP are gauged by the riboswitch which can act as a rheostat to control levels such that supply and demand are facilitated. Created with BioRender.com.

in *pACP:THIC* compared to wild type (Figure 4A). Measurement of the tissue TDP content shows that it is not significantly different between the lines (Figure 4B). Next, we measured *IS* in all lines and observed major alterations in the daily rhythms compared to wild type (Figure 4C). Although oscillation can be discerned in *pACP:THIC*, the shape of the peaks are much broader and phasing of *IS* is 5.5 h earlier than that in wild type (Figures 4C and 4D). In *pTHIC_EE_CBS:THIC*, the oscillation of *IS* is less robust and the waveform substantially different from wild type (Figure 4C). As TDP levels are similar to wild type in both cases, this suggests that cellular changes under L/D cycles cannot be appropriately gauged and there is less precision in the response of the riboswitch. Such alteration of the *THIC* promoter resulted in plants that were generally chlorotic, especially in the case of *pTHIC_EE_CBS:THIC*, and stunted in growth with reduced biomass compared to wild type under L/D cycles (Figures 4E and 4F). Indeed, these lines are morphologically similar to *NRR*. Remarkably, on the other hand, all lines were indistinguishable under LL and in terms of biomass (Figures 4E and 4F). *THIC* expression levels remained increased especially in *pTHIC_EE_CBS:THIC* under LL as for *NRR* (Figure 4G) and thus does not seem to impact growth under this condition. To test if the increased levels of *THIC* expression could negatively impact plant fitness particularly under the dark period of LD, we grew plants under LL and transferred them to continuous dark for 3 days followed by reillumination. Photographs did not indicate major differences in the morphology between the lines during this regime (Figure S8). We measured the maximum potential quantum efficiency of photosystem II (F_v/F_m) before and during the dark period as well as upon light re-exposure (recovery). Indeed, F_v/F_m is significantly lower for *NRR* as well as the *pTHIC_EE_CBS:THIC* lines during the dark and gradually recovers upon reillumination (Figure S9). Therefore, accumulation of the THIC protein could have a negative impact on the plant during the dark period.

Taking everything together, we conclude that phasing *THIC* transcript expression to the right time of day is important and suggests that the circadian clock regulation is important for the riboswitch to robustly gauge its response to TDP levels particularly under L/D cycles. As a corollary, coupling between the circadian clock and the riboswitch is critical to appropriately regulate *THIC* transcript levels in response to the requirements for TDP, which is essential for plant growth and health under environmental cycles. Misregulation of *THIC* expression and its accumulation can negatively impact plant growth most likely during the dark phase of LD cycles.

Conclusive comments

Here a comparison of riboswitch mutants with plants engineered to overexpress the biosynthesis *de novo* pathway genes *THIC* and *THI1* (*TTOE*) allows us to refine the importance of the riboswitch in responding to TDP levels over L/D cycles. Firstly, both *TTOE* and riboswitch mutants have enhanced levels of TDP, the former due to a balanced increase in the key biosynthesis regulatory genes, and the latter due to the loss of negative feedback control on *THIC* expression. However, in contrast to the chlorotic stunted riboswitch mutants, *TTOE* appears morphologically normal under L/D. Of importance is that riboswitch mutants do not retain daily oscillation of *THIC* expression, but rather constitutive enhanced expression is observed, whereas *TTOE* retains daily regulation of *THIC* expression. In the riboswitch mutants, the corresponding expected imbalance in thiamine pyrimidine precursor provision cannot be compensated by supplying the thiazole moiety. Similarly, the possible inappropriate hoarding of iron by THIC at the detriment of other proteins is not alleviated by supplying iron. Furthermore, any alteration of circadian clock operation does not account for differences between riboswitch mutants and *TTOE*. Rather, *TTOE* appears to adapt to modestly enhanced TDP levels through a gauged response of the riboswitch, as evidenced by increased splicing in the 3′-UTR of *THIC*, which cannot happen in riboswitch mutants. As noted earlier, the riboswitch response is within the nucleus and how coenzyme status is communicated is not yet known. One could speculate that a message could be relayed by a metabolite derivative of a TDP-dependent process that signifies coenzyme sufficiency or deficiency and would be adaptive to the cellular needs as a function of its environment akin to a retrograde signal. Furthermore, although we did not observe a significant impact on the clock in this study, that is not to say that the oscillator is not affected under alternative situations. More extreme ranges of TDP coenzyme sufficiency or deficiency under particular environmental circumstances may influence the oscillator, directly or indirectly adjusting period, phase, or amplitude to

anticipate and preprogram the response to the new cellular circumstance. Exploring such circumstances is a fertile future research area and would provide insight into the relevance of coenzymes in shaping metabolic homeostasis and its connection to the oscillator. We show that phasing of *THIC* expression to the right time of day is important as engineering plants with peak *THIC* transcript phased to a different time of day results in unhealthy plants under LD cycles and is linked to imprecision in the response of the riboswitch. It's possible that distinct phases of biosynthesis and transporter expression, for example, are important for allowing the riboswitch to gauge its response to TDP levels, particularly under L/D cycles (Figure 4I). In support of this hypothesis, riboswitch mutants are indistinguishable from *TTOE* or wild type under LL conditions during which metabolic reprograming does not occur and strict monitoring of TDP levels would not be deemed critical. Our data demonstrate that clock and riboswitch control of *THIC* in tandem are essential for appropriate gauging of TDP levels under L/D cycles in Arabidopsis. Given that all transgenic lines perform like wild type under LL conditions and the daily rhythm of intron splicing is a function of L/D cycles,[5] then communication of TDP status through the riboswitch is highly important under environmental cycles. Under L/D cycles, the maximum level of "TDP_{free}" is during the day and thus represents the time when supply surpasses demand. Gauging supply during the day may be crucial based on several observations: firstly, it was recently suggested that TDP might purposely be curtailed during the day to limit respiratory flux when light serves as a sufficient energy source for plants[11]; secondly, sensing of TDP levels is critical for the metabolic reprograming that occurs upon changes in photoperiod and the corresponding change in the timing of the L/D transition[3]; and thirdly, in riboswitch-disabled plants increased pools of TDP-dependent enzyme activities were concomitant with inappropriate enhanced respiration due to overoxidation of carbon through the trichloroacetic acid (TCA) cycle leading to starvation before the end of the night.[15] While both *NRR* and *TTOE* have enhanced tissue levels of TDP, accurate gauging of levels appears to be in place in the latter as evidenced by the diurnal increased riboswitch activity. This may serve to regulate overall expression of *THIC* in *TTOE* to be similar to wild type. By contrast, *NRR* lines are unable to gauge TDP levels, and the result is constitutive overexpression of *THIC*. Phasing of the riboswitch response relative to the L/D transition is also important as the developmental phenotype of the altered timing of *THIC* expression indicates. This is not merely a consequence of differences in *THIC* expression levels *per se* as the plants behave like wild type under constant environmental conditions. The study highlights the importance of the riboswitch and provides an important rationale for its conservation in plant species and function under L/D cycles. Furthermore, the fact that plants can accommodate enhanced levels of TDP is important for ongoing efforts to improve nutrient content as well as an understanding of its impacts on general plant fitness.

STAR★METHODS

Detailed methods are provided in the online version of this paper and include the following:

- KEY RESOURCES TABLE
- RESOURCE AVAILABILITY
  - Lead contact
  - Materials availability
  - Data and code availability
- EXPERIMENTAL MODEL AND SUBJECT DETAILS
  - Plant material and growth conditions
- METHOD DETAILS
  - Gene expression analysis by RT-qPCR
  - Protein extraction and immunochemical analyses
  - B_1 vitamer quantification by HPLC
  - Measurements of photosynthetic efficiency
- QUANTIFICATION AND STATISTICAL ANALYSIS

SUPPLEMENTAL INFORMATION

Supplemental information can be found online at https://doi.org/10.1016/j.isci.2023.106134.

ACKNOWLEDGMENTS

We gratefully acknowledge the Swiss National Science Foundation (grants 31003A-141117/1 and 31003A_162555/1 to T.B.F.), as well as the University of Geneva for supporting this work. We are grateful to Céline Roux for preliminary HPLC investigations during the course of this study. We thank Asaph Aharoni

(Weizmann Institute of Science, Israel) for providing the *RR1* and *NRR1* lines and Aymeric Goyer (Oregon State University, U.S.A.) for the *TTOE* lines and the THI1 antibody. We thank Marco Mellon (University of Geneva) for assistance with photosynthetic performance assays.

AUTHOR CONTRIBUTIONS

T.B.F. conceived the study; Z.N., L.L., and C.T. performed most of the work; K.W. contributed HPLC analysis; I.D. and M. de M. assisted with plant work and analyzed data; T.B.F. wrote the article with assistance from Z.N., L.L., and C.T.

DECLARATION OF INTERESTS

The authors declare no competing interests.

Received: July 6, 2022
Revised: December 3, 2022
Accepted: January 31, 2023
Published: February 3, 2023

REFERENCES

1. Stitt, M., and Gibon, Y. (2014). Why measure enzyme activities in the era of systems biology? Trends Plant Sci. *19*, 256–265.

2. Cheung, C.Y.M., Poolman, M.G., Fell, D.A., Ratcliffe, R.G., and Sweetlove, L.J. (2014). A diel flux balance model captures interactions between light and dark metabolism during day-night cycles in C3 and crassulacean acid metabolism leaves. Plant Physiol. *165*, 917–929.

3. Rosado-Souza, L., Proost, S., Moulin, M., Bergmann, S., Bocobza, S.E., Aharoni, A., Fitzpatrick, T.B., Mutwil, M., Fernie, A.R., and Obata, T. (2019). Appropriate thiamin pyrophosphate levels are required for acclimation to changes in photoperiod. Plant Physiol. *180*, 185–197.

4. Fitzpatrick, T.B., and Noordally, Z. (2021). Of clocks and coenzymes in plants: intimately connected cycles guiding central metabolism? New Phytol. *230*, 416–432.

5. Noordally, Z.B., Trichtinger, C., Dalvit, I., Hofmann, M., Roux, C., Zamboni, N., Pourcel, L., Gas-Pascual, E., Gisler, A., and Fitzpatrick, T.B. (2020). The coenzyme thiamine diphosphate displays a daily rhythm in the Arabidopsis nucleus. Commun. Biol. *3*, 209.

6. Hanson, A.D., Amthor, J.S., Sun, J., Niehaus, T.D., Gregory, J.F., 3rd, Bruner, S.D., and Ding, Y. (2018). Redesigning thiamin synthesis: prospects and potential payoffs. Plant Sci. *273*, 92–99.

7. McCourt, J.A., Nixon, P.F., and Duggleby, R.G. (2006). Thiamin nutrition and catalysis-induced instability of thiamin diphosphate. Br. J. Nutr. *96*, 636–638.

8. Chatterjee, A., Abeydeera, N.D., Bale, S., Pai, P.J., Dorrestein, P.C., Russell, D.H., Ealick, S.E., and Begley, T.P. (2011). *Saccharomyces cerevisiae* THI4p is a suicide thiamine thiazole synthase. Nature *478*, 542–546.

9. Li, L., Nelson, C.J., Trösch, J., Castleden, I., Huang, S., and Millar, A.H. (2017). Protein degradation rate in *Arabidopsis thaliana* leaf growth and development. Plant Cell *29*, 207–228.

10. Sun, J., Sigler, C.L., Beaudoin, G.A.W., Joshi, J., Patterson, J.A., Cho, K.H., Ralat, M.A., Gregory, J.F., 3rd, Clark, D.G., Deng, Z., et al. (2019). Parts-prospecting for a high-efficiency thiamin thiazole biosynthesis pathway. Plant Physiol. *179*, 958–968.

11. Joshi, J., Folz, J.S., Gregory, J.F., 3rd, McCarty, D.R., Fiehn, O., and Hanson, A.D. (2019). Rethinking the PDH bypass and GABA shunt as thiamin-deficiency workarounds. Plant Physiol. *181*, 389–393.

12. Sudarsan, N., Barrick, J.E., and Breaker, R.R. (2003). Metabolite-binding RNA domains are present in the genes of eukaryotes. RNA *9*, 644–647.

13. Bocobza, S., Adato, A., Mandel, T., Shapira, M., Nudler, E., and Aharoni, A. (2007). Riboswitch-dependent gene regulation and its evolution in the plant kingdom. Genes Dev. *21*, 2874–2879.

14. Wachter, A., Tunc-Ozdemir, M., Grove, B.C., Green, P.J., Shintani, D.K., and Breaker, R.R. (2007). Riboswitch control of gene expression in plants by splicing and alternative 3′ end processing of mRNAs. Plant Cell *19*, 3437–3450.

15. Bocobza, S.E., Malitsky, S., Araújo, W.L., Nunes-Nesi, A., Meir, S., Shapira, M., Fernie, A.R., and Aharoni, A. (2013). Orchestration of thiamin biosynthesis and central metabolism by combined action of the thiamin pyrophosphate riboswitch and the circadian clock in Arabidopsis. Plant Cell *25*, 288–307.

16. Kong, D., Zhu, Y., Wu, H., Cheng, X., Liang, H., and Ling, H.Q. (2008). At*THIC*, a gene involved in thiamine biosynthesis in *Arabidopsis thaliana*. Cell Res. *18*, 566–576.

17. Raschke, M., Bürkle, L., Müller, N., Nunes-Nesi, A., Fernie, A.R., Arigoni, D., Amrhein, N., and Fitzpatrick, T.B. (2007). Vitamin B1 biosynthesis in plants requires the essential iron–sulfur cluster protein, THIC. Proc. Natl. Acad. Sci. USA *104*, 19637–19642.

18. Dong, W., Stockwell, V.O., and Goyer, A. (2015). Enhancement of thiamin content in *Arabidopsis thaliana* by metabolic engineering. Plant Cell Physiol. *56*, 2285–2296.

19. Martinis, J., Gas-Pascual, E., Szydlowski, N., Crèvecoeur, M., Gisler, A., Bürkle, L., and Fitzpatrick, T.B. (2016). Long-distance transport of thiamine (vitamin B1) is concomitant with that of polyamines. Plant Physiol. *171*, 542–553.

20. Kamioka, M., Takao, S., Suzuki, T., Taki, K., Higashiyama, T., Kinoshita, T., and Nakamichi, N. (2016). Direct repression of evening genes by CIRCADIAN CLOCK-ASSOCIATED1 in the Arabidopsis circadian clock. Plant Cell *28*, 696–711.

21. Nagel, D.H., Doherty, C.J., Pruneda-Paz, J.L., Schmitz, R.J., Ecker, J.R., and Kay, S.A. (2015). Genome-wide identification of CCA1 targets uncovers an expanded clock network in Arabidopsis. Proc. Natl. Acad. Sci. USA *112*, E4802–E4810.

22. Moulin, M., Nguyen, G.T., Scaife, M.A., Smith, A.G., and Fitzpatrick, T.B. (2013). Analysis of Chlamydomonas thiamin metabolism in vivo reveals riboswitch plasticity. Proc. Natl. Acad. Sci. USA *110*, 14622–14627.

23. Pourcel, L., Moulin, M., and Fitzpatrick, T.B. (2013). Examining strategies to facilitate vitamin B1 biofortification of plants by genetic engineering. Front. Plant Sci. *4*, 160.

24. Atilho, R.M., Mirihana Arachchilage, G., Greenlee, E.B., Knecht, K.M., and Breaker, R.R. (2019). A bacterial riboswitch class for the thiamin precursor HMP-PP employs a terminator-embedded aptamer. Elife *8*, e45210.

25. Li, S.L., and Rédei, G.P. (1969). Thiamine mutants of the crucifer, Arabidopsis. Biochem. Genet. *3*, 163–170.

26. Chabregas, S.M., Luche, D.D., Farias, L.P., Ribeiro, A.F., van Sluys, M.A., Menck, C.F., and Silva-Filho, M.C. (2001). Dual targeting properties of the N-terminal signal sequence of *Arabidopsis thaliana* THI1 protein to mitochondria and chloroplasts. Plant Mol. Biol. *46*, 639–650.

27. Braymer, J.J., Freibert, S.A., Rakwalska-Bange, M., and Lill, R. (2021). Mechanistic concepts of iron-sulfur protein biogenesis in Biology. Biochim. Biophys. Acta. Mol. Cell Res. *1868*, 118863.

28. Guerinot, M.L. (1994). Microbial iron transport. Annu. Rev. Microbiol. *48*, 743–772.

29. Vert, G., Grotz, N., Dédaldéchamp, F., Gaymard, F., Guerinot, M.L., Briat, J.F., and Curie, C. (2002). IRT1, an Arabidopsis transporter essential for iron uptake from the soil and for plant growth. Plant Cell *14*, 1223–1233.

30. Fejes, E., Pay, A., Kanevsky, I., Szell, M., Adam, E., Kay, S., and Nagy, F. (1990). A 268 bp upstream sequence mediates the circadian clock-regulated transcription of the wheat *Cab-1* gene in transgenic plants. Plant Mol. Biol. *15*, 921–932.

31. Millar, A.J. (2016). The intracellular dynamics of circadian clocks reach for the light of ecology and evolution. Annu. Rev. Plant Biol. *67*, 595–618.

32. Nakamichi, N., Kiba, T., Henriques, R., Mizuno, T., Chua, N.H., and Sakakibara, H. (2010). PSEUDO-RESPONSE REGULATORS 9, 7, and 5 are transcriptional repressors in the Arabidopsis circadian clock. Plant Cell *22*, 594–605.

33. Zielinski, T., Moore, A.M., Troup, E., Halliday, K.J., and Millar, A.J. (2014). Strengths and limitations of period estimation methods for circadian data. PLoS One *9*, e96462.

34. Gerdes, S., Lerma-Ortiz, C., Frelin, O., Seaver, S.M.D., Henry, C.S., de Crécy-Lagard, V., and Hanson, A.D. (2012). Plant B vitamin pathways and their compartmentation: a guide for the perplexed. J. Exp. Bot. *63*, 5379–5395.

35. Michael, T.P., and McClung, C.R. (2002). Phase-specific circadian clock regulatory elements in Arabidopsis. Plant Physiol. *130*, 627–638.

36. Clough, S.J., and Bent, A.F. (1998). Floral Dip: a simplified method for Agrobacterium-mediated transformation of *Arabidopsis thaliana*. Plant J. *16*, 735–743.

37. Murashige, T., and Skoog, F. (1962). A revised medium for rapid growth and bio assays with tobacco tissue cultures. Physiol. Plant. *15*, 473–497.

38. Bradford, M.M. (1976). A rapid and sensitive method for the quantitation of microgram quantities of protein utilizing the principle of protein-dye binding. Anal. Biochem. *72*, 248–254.

STAR★METHODS

KEY RESOURCES TABLE

REAGENT or RESOURCE	SOURCE	IDENTIFIER
Antibodies		
A. thaliana THIC rabbit primary antibody	In house	N/A
A. thaliana THI1 rabbit primary antibody	Dong et al.[18]	N/A
Goat anti-rabbit IgG HRP conjugate secondary antibody	Biorad	AS09602
Mouse monoclonal anti-actin (plant) primary antibody	Sigma	A0480
Goat anti-mouse IgG HRP conjugate secondary antibody	Biorad	Cat#170-6516
Bacterial and virus strains		
Agrobacterium tumefaciens C58	In house stock	N/A
Chemicals, peptides, and recombinant proteins		
Murashige & Skoog Medium, basal salt mixture	Duchefa	Cat#M0221.0050
2-(MN-morpholino)-ethane sulfonic acid (MES)	Sigma-Aldrich	Cat#G-8529
BASTA	Bayer Group	Cat#06470033
4-methyl-5-thiazoleethanol (HET)	Sigma-Aldrich	Cat#190675-25G
Thiamine hydrochloride	Sigma-Aldrich	Cat#T4625
Sequestrene	Syngenta	Cat#2843
Agar	Duchefa	Cat#p1001.1000
RNase-free DNase	Qiagen	Cat#79254
PowerUp SYBR Green master mix	Applied Biosystems	Cat#A25743
Sodium phosphate monobasic	Acros	Cat#271750010
Sodium phosphate dibasic	ThermoFisher Scientific	Cat#271060010
β-mercaptoethanol	Gibco	Cat#21985-023
EDTA	Sigma-Aldrich	Cat#EDFS-100G
Triton X-100	Merck	Cat#11869
Protease Inhibitor Cocktail for plant cell extracts	Sigma-Aldrich	Cat#P9599
Protein Assay Dye Reagent Concentrate	Bio-Rad	Cat#5000006
Bovine Serum Albumin (BSA)	Sigma-Aldrich	Cat#P0914
Tween-20	Applichem	Cat#A1389.0500
Trizma acetate	Fluka	Cat#93337
Trichloroacetic acid (TCA)	Sigma-Aldrich	Cat#T6399
Hydrochloric acid	Fisher Chemical	Cat#H/1150/PB15
Magnesium chloride hexahydrate	Sigma-Aldrich	Cat#M9272-500G
Potassium Ferricyanide (III)	Sigma-Aldrich	Cat#244023-100G
Sodium Hydroxide	Acros	Cat#206060010
Methanol, HPLC grade	Fisher Scientific	Cat#M/4058/17
Thiamine monophosphate (TMP)	Sigma-Aldrich	Cat#T8637
Thiamine diphosphate (TDP)	Sigma-Aldrich	Cat#C8754
Potassium phosphate monobasic	Sigma-Aldrich	Cat#P0662
Di-potassium hydrogen phosphate	Fluka	Cat#60355
KpnI	New England	Cat#R3142S
NcoI	New England	Cat#R3193S
XmaI	New England	Cat#R0180S

(*Continued on next page*)

Continued

REAGENT or RESOURCE	SOURCE	IDENTIFIER
Critical commercial assays		
RNA NucleoSpin Plant kit	Macherey-Nagel	Cat#740949.250
SuperScript III reverse transcriptase	Life Technologies	Cat#18064014
oligo(dT)15 primers	Promega	Cat#C110A
iBlot Transfer Stack, Nitrocellulose	ThermoFisher Scientific	Cat#IB301032
SNAP i.d. 2.0 Midi Blot Holders	Millipore	Cat#SNAP2BHMN0100
WesternBright ECL-HRP substrates	Witec AG	Cat#K-12045-D50
Hypersil BDS Phenyl 120Å 5 µm guard cartridge 2.0 x 10 mm pre-column	Thermoscientific	Cat#28905-154630
Cosmosil π NAP 2.0 ID x 150 mm column	Nacalai Tesque Inc.	Cat#08078-41
Experimental models: Organisms/strains		
Arabidopsis thaliana: Columbia-0	In house stock	N/A
Arabidopsis *thiC1-1*	In house stock[17]	SAIL_793_H10 (N835499)
Arabidopsis *thiC1-2*	European Arabidopsis Stock Center	SALK_011114 (N511114)
Arabidopsis *tz-1*	European Arabidopsis Stock Center	N3375
Arabidopsis *RR1*	Bocobza et al.[15]	N/A
Arabidopsis *NRR1*	Bocobza et al.[15]	N/A
Arabidopsis *RR2* (L2)	This study	N/A
Arabidopsis *NRR2* (L2, L7, L11)	This study	N/A
Arabidopsis *TTOE* (L7.3, L7.5, L8)	Dong et al. [18]	N/A
Arabidopsis *ACP4*	This study	N/A
Arabidopsis *EE_CBS*	This study	N/A
Oligonucleotides		
Primers (Table S2)	This study	N/A
Recombinant DNA		
pTHIC::THIC-RR	Bocobza et al.[15]	N/A
pTHIC::THIC-NRR	Bocobza et al.[15]	N/A
pTHIC EE_CBS::THIC	This study	N/A
pACP4::THIC	This study	N/A
Software and algorithms		
Graphpad Prism v7	Graphpad	https://www.graphpad.com/scientific-software/prism/
BioDare2	Zielinski et al.[33]	https://biodare2.ed.ac.uk
QuantStudio™ Design & Analysis Software v1.4.3	Thermo Fisher	https://www.thermofisher.com/ch/en/home/global/forms/life-science/quantstudio-3-5-software.html
FluorCam7	Photon Systems Instruments	https://fluorcams.psi.cz/products/open-fluorcam/#download
Amersham Imager 680 web tool	Thermo Fischer	https://www.thermofisher.com/ch/en/home/technical-resources/software-downloads/ibright-western-imager.html
1260-FLD	Agilent	N/A

RESOURCE AVAILABILITY

Lead contact

Further questions and request for resources should be directed to the lead contact Teresa B. Fitzpatrick (theresa.fitzpatrick@unige.ch).

Materials availability

Requests for resources should be directed to the lead contact.

Data and code availability

- All data reported in this study will be shared by the lead contact upon request.
- This paper does not report original code.
- Any additional information required to reanalyse the data reported in this paper is available from the lead contact upon request.

EXPERIMENTAL MODEL AND SUBJECT DETAILS

Plant material and growth conditions

All lines were in the *Arabidopsis thaliana* Col-0 ecotype background (wild type) and are listed in Table S1. *Arabidopsis thaliana* SAIL_793_H10 (N835499) referred to here as *thiC1-1* was from an in house stock.[17] SALK_011114 (N511114) referred to here as *thiC1-2* and *tz-1* (N3375,[25]) were obtained from the European Arabidopsis Stock Center. The *irt1-2* line was donated by Marie Barberon (University of Geneva). Three independent lines of Arabidopsis carrying the *p35S::THI1 pUBI1::THIC* construct, referred to here as *TTOE* (L7.3, L7.5 and L8) were donated by Aymeric Goyer, Oregon State University.[18] The *thiC1-2* plants carrying either the *pTHIC:THIC:RR* or *pTHIC:THIC:NRR* construct, in which *THIC* is expressed under the control of its upstream region relative to the start codon (−1584 to −1 bp) and region downstream of the stop codon including 3′-UTR (2176 to 3581 bp relative to the start codon) with either a Responsive Riboswitch (plants referred to as *RR1*) or Non-Responsive Riboswitch (plants referred to as *NRR1*), which bears a A515G mutation relative to the *THIC* stop codon in the *THIC* 3′-UTR and were donated by Asaph Aharoni, Weizmann Institute of Science.[15] Additionally, we generated independent transgenic lines in the *thiC1-1* background carrying either the *pTHIC:THIC:RR* or *pTHIC:THIC:NRR* construct. The constructs were introduced into *Agrobacterium tumefaciens* strain C58 and used to transform *thiC1-1* by the floral dip method.[36] For the selection of lines, T1 seedlings were sprayed with 55 mg/L of glufosinate at 5 days and 8 days after germination (DAG) and selection was maintained at 25 μg ml^{-1} in sterile culture. These lines are referred to as *RR2* (L2) and *NRR2* (L2, L7 and L11) in this study. As the *thiC1-1* T-DNA insertion line and the vector contained the same glufosinate resistance, plant selection was possible due to the thiamine auxotrophy of the *thiC* background. The altered promoter lines were generated by either substituting the *THIC* upstream region in *pTHIC:THIC:RR* with that of *ACP4* (At4g25050, -688 to +172 bp) using the *KpnI* and *Xma1* restriction sites (see Table S2 for primers used) or by altering the promoter located evening element (AAATATCT) in *THIC* to the CIRCADIAN CLOCK ASSOCIATED 1-binding site (CBS) element (AAAAATCT) using site-directed mutagenesis (see Table S2 for primers used). Primers for genotyping are given in Table S2. Plants were either grown on soil in CLF Grobank chambers (Plant Climatics, Germany) or in sterile culture in MLR-352 environmental test chambers (Sanyo Electric) under 8 hr L/16 hr D, 12 hr L/12 hr D or 16 hr L/8 hr D photoperiods or continuous light (LL) as indicated. Light intensity was 120–140 μmol photons m^{-2} s^{-1}, relative humidity was ~70%, and temperature was maintained at 20°C. For supplementation experiments, plants on soil were watered and leaves were sprayed either with water (control) or 100 μM 4-methyl-5-thiazole ethanol 98% (HET), or 100 μM thiamine-HCl, or watered with 0.5 g/L Sequestrene, as indicated. Seeds grown in sterile culture were surface sterilized, stratified for 4 days at 4°C in the dark, grown on half-strength Murashige and Skoog (MS) medium[37] pH 5.7, without sucrose in 0.55% (w/v) agar plates. For tissue gene expression, B_1 vitamer quantification and protein extraction in rosette leaves, shoot material was collected at 28 DAG from plants grown on soil under a 12 hr L/12 hr D photoperiod. Material was harvested in biological triplicates each consisting of a pool of five plants. For photosynthetic performance assays, plants were grown on soil in LL for 21 days. Their photosynthetic efficiency was measured before being transferred to constant dark (DD) conditions for 3 days. Photographs were taken every 24 hr and their photosynthetic capacities were monitored. After the dark treatment, plants were brought back to LL conditions, and they were similarly monitored for the following 3 days for their recovery capacity. Two leaves of three plants were assessed for each genotype. For time series experiments, plants were grown in sterile culture and

split-entrained in diel cycles of 12 hr L/12 hr D or 12 hr D/12 hr L at a light intensity of approximately 120 μmol m^{-2} s^{-1} and at a constant temperature of 20°C. At dawn (0 hr) 13 DAG, plants were either kept in diel cycles of light and dark (diurnal conditions) or transferred to LL (circadian free-running conditions). From dawn/subjective dawn at 14 DAG shoot material was harvested at 4 hr intervals, at the times indicated, for 3 days in biological triplicates, each consisting of material from ten plants. All harvested tissue was immediately frozen in liquid nitrogen and maintained at −80°C until analysis. Frozen tissue was crushed and mixed before ~50 mg was taken (note that the exact tissue mass for each sample was recorded to normalize the extraction volumes and the data in the HPLC method). The frozen plant material was ground to a fine powder using 2 mm Ø glass beads (Huberlab) and a TissueLyser (Qiagen) for 1 min at maximum frequency. For fresh weight biomass measurements, shoot material was harvested in biological triplicates each consisting of a pool of five plants and weighed on a precision balance (Kern ABS).

METHOD DETAILS

Gene expression analysis by RT-qPCR

Total RNA was extracted using the RNA NucleoSpin Plant kit following the manufacturer's instructions and treated with RNase-free DNase to remove trace genomic DNA. Reverse transcription of 1 μg RNA into cDNA was performed using Superscript III reverse transcriptase and oligo(dT)15 primers according to the manufacturer's instructions. Fluorescence-based quantitative real time Reverse Transcriptase-PCR analyses were performed in 384-well plates using a QuantStudio5 instrument and PowerUp SYBR Green master mix. The following amplification program was used: 10 min denaturation at 95°C followed by 40 cycles of 95°C for 15 s and 60°C for 1 min. Data were analyzed using the comparative cycle threshold method (2−ΔCT) and normalized to the reference gene *UBC21* (At5g25760). Primers used are listed in Table S2. Each experiment was performed with at least three biological and three technical replicates.

Protein extraction and immunochemical analyses

Total protein was extracted from 100 mg of homogenized plant tissue with 300 μl of extraction buffer (50 mM sodium phosphate buffer, pH 7.0, containing 5 mM β-mercaptoethanol, 10 mM EDTA, 0.1% Triton X-100 [v/v] and freshly added 1% [v/v] protease inhibitor cocktail for plant cell extracts). Samples were kept on ice and vortexed for 1 min and centrifuged for 10 min at 16,000 *g* at 4°C and the supernatant containing the total protein extract was transferred to a fresh tube. Total protein content was determined using the Bradford method,[38] following the manufacturer's recommendations (Bio-Rad), and using standard curves derived from known concentrations of bovine serum albumin. Linearity was observed from 0 to 1.5 μg and samples from plant extractions were diluted five-fold with extraction buffer to have a final protein concentration in this range. Twenty μg of total protein extract were loaded and separated by SDS-PAGE on 12% polyacrylamide gels. Migrated proteins were transferred to a nitrocellulose membrane using an iBlot system and immunodetection was performed using the SNAP i.d. 2.0 system using a 1:1000 dilution of an *A. thaliana* THIC rabbit primary antibody generated in house[17] or an *A. thaliana* THI1 rabbit primary antibody donated by Aymeric Goyer, Oregon State University[18] and a 1:3000 dilution of goat anti-rabbit IgG horseradish peroxidase (HRP) conjugate secondary antibody. Chemiluminescence was detected using WesternBright ECL and captured using an Amersham Imager 680. The membranes were washed with Tris buffered saline containing 0.1% Tween-20 and probed again for protein loading control using a 1:10,000 dilution of mouse monoclonal anti-actin (plant) primary antibody and a 1:3000 dilution of goat anti-mouse IgG HRP conjugate.

B_1 vitamer quantification by HPLC

B_1 vitamer content was determined essentially as described in[5] with some modifications. Vitamin B_1 was extracted at a 1:2 ratio of mg tissue to 1% TCA (v/v), typically 50 mg of homogenized plant tissue was re-suspended in 100 μl 1% TCA. Samples were vortexed for 10 min at room temperature and centrifuged for 15 min at 16000 *g* at room temperature (ca. 22°C) to remove precipitated proteins. The supernatant was adjusted with 1 M Tris-HCl, pH 9.0, containing 50 mM magnesium chloride (10% v/v). Derivatization of thiamine and its phosphorylated forms to their corresponding thiochromes was achieved by alkaline oxidation, whereby 7 μl of freshly made 46 mM potassium ferricyanide (in 23% sodium hydroxide (w/v)) was added to 56 μl of extracts, vortexed and then incubated in complete darkness for 10 min. Twelve μl of 1 M sodium hydroxide and 25 μl of methanol were then added to the extracts, vortexed and then clarified by centrifugation prior to analysis. Quantification of the B_1 vitamers was performed in the linear range of a standard curve constructed with known amounts of each vitamer using an Agilent 1260 Infinity series HPLC furnished

with a binary pump, an autosampler and a fluorometer. A Hypersil BDS Phenyl 120Å 5 μm guard cartridge 2.0 × 10 mm pre-column was used to protect the column from mobile phase contamination. A Cosmosil π NAP 2.0 ID x 150 mm column was used for stationary phase separation of the B_1 vitamers. Mobile phase A was 50 mM potassium phosphate buffer, pH 7.2 and mobile phase B was 100% methanol HPLC grade. The following conditions were used: flow, 0.5 ml/min; temperature, 35°C; fluorimetry detection excitation 375 nm, emission 450 nm; PMT gain, 18; peak width, > 0.2 min, 4 s response time, 2.31 Hz; injection volumes, 1 μl and 10 μl; equilibration conditions, 89% buffer A and 11% buffer B. The 20 min running conditions used the following mixtures of buffers A and B; 0 min, 89% buffer A and 11% buffer B; 9.5 min, 68% buffer A and 32% buffer B; 13 min, 40% buffer A and 60% buffer B; 13.5 min, 100% buffer B; 15.5 min, 100% buffer B; 16 min, 89% buffer A and 11% buffer B and 20 min, 89% buffer A and 11% buffer B. Resultant chromatograms were subject to peak integration to quantify B_1 vitamers present in the plant extracts. Statistical relevance was performed using GraphPad Prism v7.

Measurements of photosynthetic efficiency

Plants previously subjected to light conditions were dark-adapted for 30 min and the maximum quantum efficiency of PSII was measured with a Fluorcam using blue actinic (470 nm) LEDs for excitation and was calculated as $F_v/F_m = (F_m - F_0)/F_m$, where F_m is the maximal fluorescence and F_0 the minimal fluorescence in the dark-adapted state. During quenching kinetic analysis, F_0 was determined after a dark period of 2 s. Then, an actinic light pulse of 1000 ms was used to determine the F_m, from which the variable fluorescence F_v was calculated. A dark relaxation period of 15 s was applied before proceeding to the induction of the Kautsky effect, which was performed using 5 saturating actinic light pulses over the course of 60 s. The peak fluorescence F_p after each pulse was measured, as well as before the last saturating light pulse (F_t). Following the very last pulse, F_0 and F_m were measured again to determine the F_v in the light steady-state. Only the maximum quantum efficiency of PSII (F_v/F_m) in the dark-adapted state are reported in this study.

QUANTIFICATION AND STATISTICAL ANALYSIS

All period, phase, and amplitude estimates of circadian rhythms are based on the MESA (Maximum Entropy Spectral Analysis) algorithm in BioDare2 (biodare2.ed.ac.uk;[33]). All statistical analyses were performed in GraphPad Prism v7. The precise statistical tests and their statistical parameters can be found in the corresponding Figure legend.